Camera-based reflectivity measurement for solar thermal applications

John D. Pye[1], Clifford K. Ho[2] and Cianan A Sims[2]

[1] Australian National University, Research School of Engineering, Canberra, Australia

+61 2 6125 8778, john.pye@anu.edu.au.

[2] Sandia National Laboratories, Albuquerque, New Mexico, USA. ckho@sandia.gov

Abstract

We assess the ability of standard digital single-lens reflex cameras to provide accurate estimates of the solar-weighted reflectivity of the receiver component in CSP systems. Such reflectivity measurement would form part of the camera-based PHLUX methods earlier presented by Cliff Ho and co-workers. A 'coupon' method is evaluated in which differences in reflected pixel intensity are used to scale reflectivity from a reference sample to a new test sample. The method appears accurate to within 1.5 percentage points of reflectivity for truly grey surfaces, but considerably worse for non-grey surfaces. Additional information from an infrared camera would significantly improve accuracy of the photographic methods in those cases.

Keywords: reflectivity, reflectometer, camera, image, intensity, receiver.

1. Introduction

Tubular receivers for solar thermal power plants, specifically tower plants, are in common use, in plants such as Gemasolar and PS10 in Spain. A key performance parameter for these receivers is the reflectivity of the reflector tubes. Because of the importance of this parameter in the overall system performance, receiver tubes may be coated with anti-reflective surface coatings that minimise the reflection of the incident focussed solar radiation. The coating may in some cases fail, or be incorrectly or incompletely applied. Uncoated surfaces may oxidise, and receivers may also become soiled by dust, bird droppings and pollutants.

As a result, measurement of the receiver reflectivity (equivalently, absorptivity) is something that we want to be able to do conveniently in the field, possibly at intervals throughout the life of the plant. These receivers are large and difficult to access, so a method that will allow reflectivity to be measured by photographic methods has strong appeal. If, furthermore, the method can make use of nothing more than a standard digital single-lens reflex (DSLR) camera, then this will be simple and low-cost.

So the question to be answered by this paper is the following: can we successfully measure receiver reflectivity using a DSLR camera, and if so how accurate can it be?

2. Background

2.1 Reflectivity measurement

Measurement of reflectivity includes both specular and diffuse reflectivity as well a directional and spectral measurement. A survey of good practices for reflectivity measurement in CSP applications was completed by SolarPACES members in 2011 [1]. For the present study, a portable reflectometer from Surface Optics Corporation, the 410-Solar, was available at Sandia National Laboratories. The 410-Solar measures reflectivity in seven different wavelength bands and calculates the solar-weighted reflectivity by essentially interpolating the reflectivity from those seven sample points to the whole solar spectrum, and convolving the spectral reflectivity with a standard solar spectrum. This instrument provides both diffuse and specular reflectivity through the use of an integrating sphere incorporated in the device.

2.1. PHLUX method

Ho and Khalsa [2] outlined the PHotographic fLUX mapping method, PHLUX, in 2011. Using a standard DSLR, the method uses a photograph of the sun to calibrate the camera sensor in radiative energy terms, then

uses the camera calibration to convert a photograph of an irradiated receiver (Figure 1) into an estimated flux map. The method requires the reflectivity of the receiver to be known, since incident flux at the receiver must be inferred from reflected light from the receiver. Two methods for photographically measuring receiver reflectivity are described in this paper, described further below, but results are not presented.

Ho et al [3], at SolarPACES 2011, gave some results of an experimental evaluation of the PHLUX method. The method is shown to be able to accommodate changes in camera and filter settings and shown to be independent of the distance and angle of the camera from the target. Finally, the linearity of the camera CCD sensor is assessed.

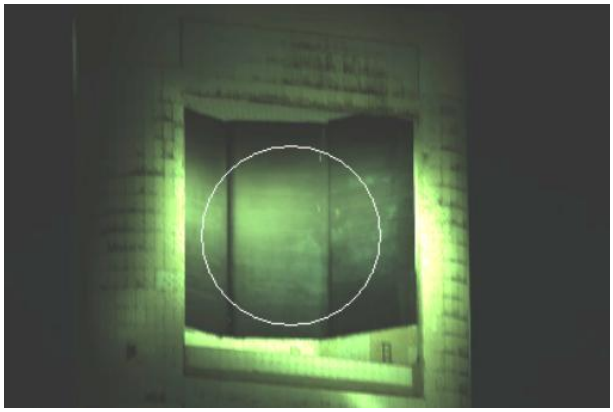

Figure 1. Photograph of a large tower receiver on-sun, with filters to avoid sensor saturation [3]. The PHLUX method aims to quantify flux on the receiver using photographs such as this one.

2.2. Reflectivity measurement by photograph

In the introductory paper about the PHLUX method, Ho and Khalsa [2] include two suggested methods for measurement of receiver reflectivity from photographs. These methods are distinct from the main PHLUX method used to determine the flux map of the concentrated radiation across the receiver, and are briefly described here.

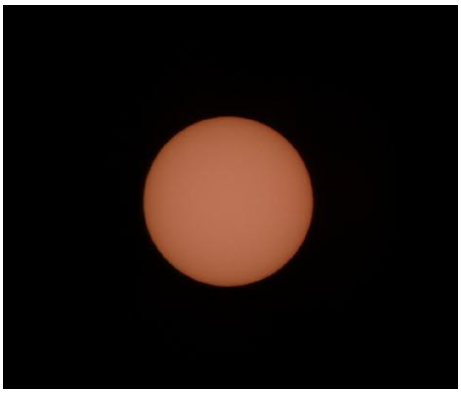

Figure 2. A photograph of the sun, taken through suitable neutral density filters, can be integrated and calibrated against a measured direct normal irradiance value. With that process, a standard camera then provides a quantitative measure of energy per sensor pixel-value increment.

In the first 'solar' method, a photograph of the sun (Figure 2) is taken and using a DNI measurement from a pyrheliometer, the camera is calibrated to give a measure of energy per measured pixel intensity, for a single colour channel from the camera's CMOS or CCD sensors. Two further photos are then taken: one of the receiver under ambient conditions and another of the receiver with a single heliostat focussed onto it. The heliostat parameters such as size, location and reflectivity must be known, so that the total flux on the receiver can be accurately calculated. The entire focal spot of the heliostat must also be incident on the

receiver surface. The integral of pixel intensities over the entire receiver surface can then be calculated for the two images, and the difference calculated. That difference, converted to an energy basis will be some fraction of the calculated incident energy from the heliostat, which will be equal to the surface reflectivity in the wavelength band of the selected colour channel, provided the surface is Lambertian. If we can assume the surface is grey, then this value will then be the solar-weighted reflectivity. The value calculated in this way is a single reflectivity number applicable for the whole receiver surface. This method cannot be used to determine a local reflectivity 'map' of the receiver surface.

In the second 'coupon' method, a single photograph is taken with a small sample 'coupon' surface of known reflectivity within the field of view, together with the receiver surface. Both of these surfaces should have similar orientation and both should be under comparable lighting conditions – we can assume they will both be under direct (1-sun) sunlight. With assumptions of the surfaces both being Lambertian and both being grey, we can use the relative intensities of pixels between the coupon and the receiver to scale the receiver reflectivity from the known reflectivity of the coupon. The method as proposed is only applied to the wavelength band of a single chosen colour channel (green was recommended); results are intended to be extrapolated to the full spectrum on the assumption that the receiver surface is grey (uniform spectral reflectivity). This method works on a pixel-by-pixel basis, allowing a reflectivity map for the entire receiver surface to be calculated. Alternatively, averaged values over a region of pixels can be used, if local variation is not needed.

In this paper, we evaluate the accuracy of the coupon method, with particular attention to the issues arising from the restricted spectral range of standard DSLR cameras.

3. Evaluation of coupon method of reflectivity measurement

3.1. Samples

To assess the accuracy of the coupon method, a sample board was prepared with a range of grey and coloured paper samples (Figure 3). Grey paper samples were newsprint from a local newspaper. Coloured paper samples were a selection of the standard sticky-notes typical in office work. These samples were chosen for their wide range of colour and (diffuse) reflectivity. In addition, one 'real' surface, a sample coated with Pyromark 2500 paint was included in the set. Pyromark 2500 is in common use as a coating for absorbers in CSP systems [4].

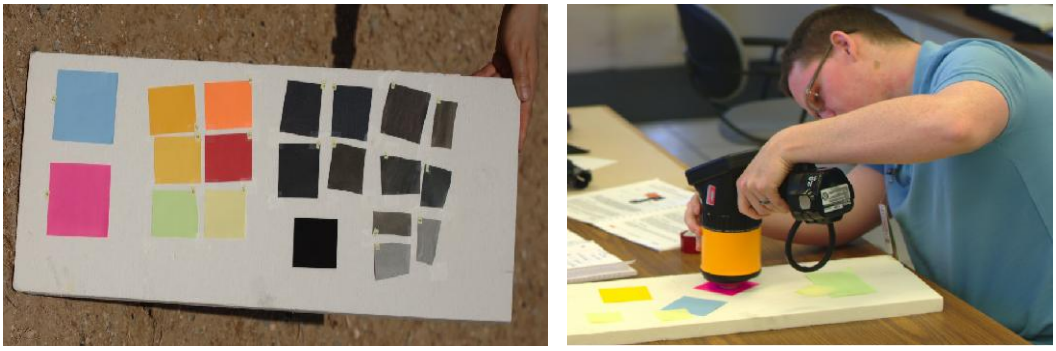

Figure 3. (a) Grey and coloured samples used to evaluate the coupon method. The very dark square is the Pyromark 2500 painted sample. (b) Measurement of the samples using the SOC 410-Solar hand-held 7-band solar reflectometer.

3.2. Characterisation with 410-Solar reflectometer

The 410-Solar was used to determine the spectral reflectivity of all of the surfaces on the sample board, including all of the paper samples as well as the Pyromark sample and the ceramic Duraboard backing. Using the data files retrieved from the 410-Solar, the spectral data for diffuse reflectivity can be extracted and plotted. The reflectivity spectra for several samples are shown in Figure 4. Wavelength ranges for the seven

detection bands of the 410-Solar are 335-380 nm, 400-540 nm, 480-600 nm, 590-720 nm, 700-1100 nm, 1000-1700 nm and 1700-2500. In this study, we assume the reflectivity to be constant within the band, and then linearly interpolate where there is a gap between bands. For the cases where the bands are overlapping, we likewise interpolate within the overlapping region. The outcome of the interpolation is shown in the red continuous lines of the upper plots of Figure 4(a)-(d).

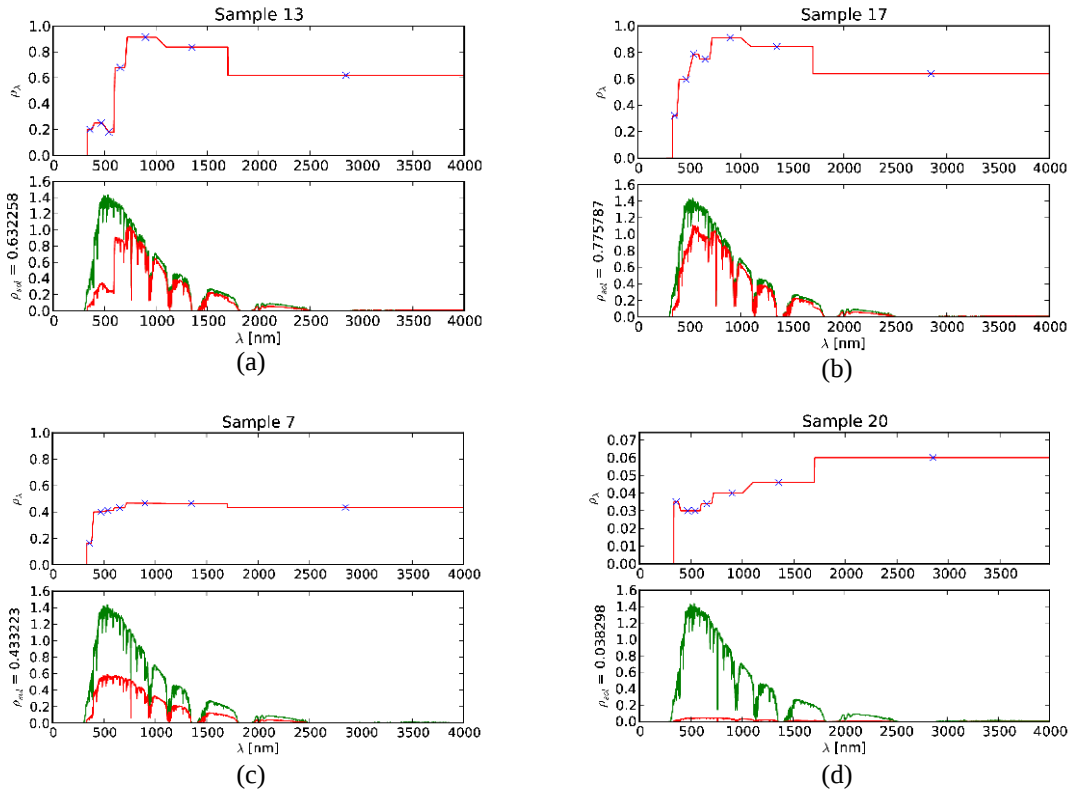

Figure 4. Reflectivity spectra from 410-Solar measurements for (a) orange paper sample (b) green paper sample (c) grey paper sample (d) Pyromark 2500 sample. The lower part of each plot shows the AM1.5 ASTM G173 air mass 1.5 solar spectrum together with the calculated reflected spectrum; at the lower left of each plot is the calculated solar-weighted reflectivity.

Once the interpolated spectral reflectivity is calculated, we use the direct+circumsolar data from reference air mass 1.5 solar spectrum, ASTM G173-03 as reported by NREL [5]. The reflectivity and solar spectrum are convolved by elementwise multiplication then integrated with respect to wavelength using Simpson's rule. The integral is then divided by the integral of the raw solar spectrum G_λ to give solar-weighted reflectivity:

$$\rho_{sol} = \frac{\int_0^\infty \rho_\lambda G_\lambda \, d\lambda}{\int_0^\infty G_\lambda \, d\lambda}$$

Values calculated for solar-weighted reflectivity from the raw spectral data by this method are in good agreement with the data calculated internally by the 410-Solar instrument.

3.2.1 Accuracy of reflectivity measurement using only visible sensors

We are ultimately interested in how well a DSLR camera could reproduce the reflectivity data from the more accurate 410-Solar instrument. The limitation of the DSLR camera is that it is designed to produce pictures using only visible components of the solar spectrum. To assess the potential errors arising from only using visible-wavelength sensors, we repeat the above calculation of solar-weighted reflectivity, but this time only using the three visible range sensors in the 410-Solar for our calculation (Figure 5).

This calculation shows that although the visible wavelengths carry a large portion of the solar energy, and as such give some estimate of the solar-weighted reflectivity, there is still a significant fraction of the solar energy in the wavelengths outside the visible range. For the grey paper sample, the reflectivity in the longer wavelengths is well approximated by that in the visible wavelengths, and the result is that prediction of reflectivity using only the visible-wavelength sensors is quite good. However for all of the other samples, which were relatively spectrally non-grey, the reflectivity estimate is quite poor.

This underlines a key problem, essentially unavoidable, with the measurement of solar-weighted reflectivity by purely visible-wavelength sensors: we don't have enough information from our sensors to do the job accurately.

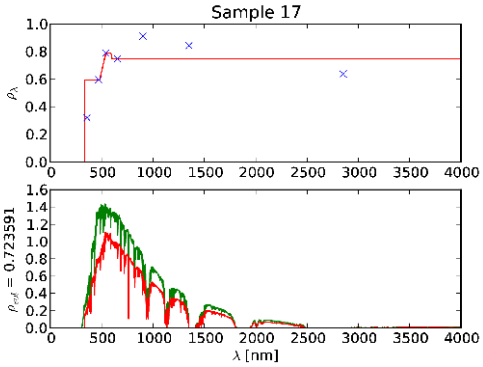

	ρ_{sol}	$\rho_{sol,vis}$
orange	0.632	0.536
green	0.776	0.724
grey	0.433	0.422
Pyromark	0.0383	0.0327

Figure 5. Left, the solar-weighted reflectivity for the green paper sample, calculated only using the visible-wavelength sensors in the 410-Solar. Right, the reflectivity data calculated from 410-Solar data with all sensors ρ_{sol} and just the visible ones $\rho_{sol,vis}$. As expected, there are significant discrepancies, in particular for the samples that are very non-grey.

3.3. Application of the coupon method to photographs

In the preceding section a simple experiment was run using only the data from the 410-Solar instrument. In this section, we implement the full coupon method, by estimating the reflectivity of 'test' samples using a single reference sample and the 410-Solar reflectivity data for that single sample.

For this comparison the pale grey paper sample, Sample 7, was chosen as the reference sample. For the Nokia D9 camera used in this experiment, raw image files can be accessed using appropriate camera settings. These images can be decoded using the open-source *dcraw* code, the output of which was incorporated into a simple PyGTK-based GUI developed for this work that shows histograms of image regions and computes average pixel intensities for the selected regions (Figure 6).

The un-normalised, un-balanced 16-bit pixel intensities from the 'raw' image files were previously shown to have good linearity with the incident irradiance at the camera, especially in the green channel [3].

To calculate the reflectivity, for this study, we use all three colour channels from the camera. The reflectivity for each channel is scaled from the spectral reflectivity measured for the corresponding colour channel from the 410-Solar, using the ratio of the pixel intensities in that same colour channel between the test sample and the reference sample,

$$\rho_{i,c} = \frac{p_{i,c}}{p_{\mathrm{ref},c}} \rho_{\mathrm{ref},c}$$

where c is one of the colour channels (blue, green or red), i is the test sample, ref is the reference sample, p is a raw, unscaled pixel intensity from the raw image file. $\rho_{\mathrm{ref},c}$ is the spectral reflectivity of the reference sample for colour channel c from the 410-Solar and $\rho_{i,c}$ is the estimated reflectivity of sample i using the coupon method.

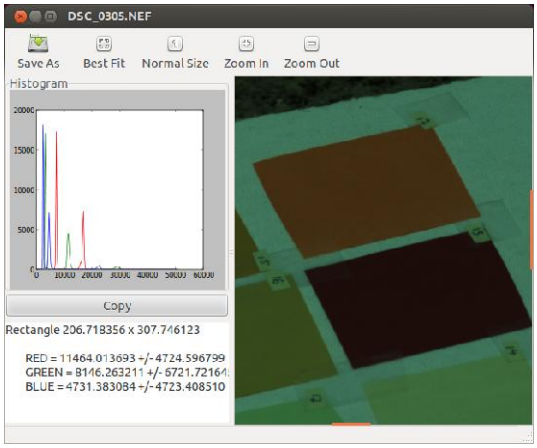

Figure 6. The average pixel value in each of the three colour channels was sampled for each coloured region from a set of raw-format (.NEF) image files from the Nikon camera.

Once we have the estimated spectral reflectivities for the three visible-wavelength colour channels, we use the same method as described in Section 3.2.1 to estimate the overall solar-weighted reflectivity.

By this method, the results shown in Figure 7 were calculated. Three different photos with variable camera position and shutter settings were used. Photo 316, in particular, was taken at approximately 45 degrees zenith angle from the sample board, and appears to show poor agreement because of that. The grey samples show quite good agreement with reflectivity measured by the 410-Solar (within 7 percentage points across all

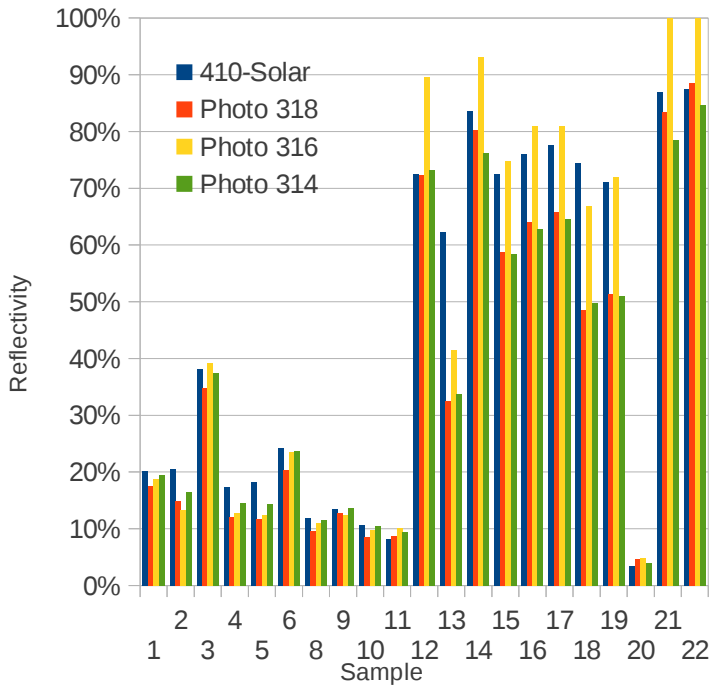

Figure 7. Solar-weighted reflectivity for all samples in the experiment calculated from several different photos, using pale grey paper sample as the reference (Sample 7), with comparison to 410-Solar results. The first bar in each group is the 410-Solar result. Samples 1-11 are all grey-coloured paper and are in quite good agreement with the 410-Solar. Samples 12-19 are coloured paper samples, and agree quite poorly. Sample 20 is the Pyromark 2500 and Samples 21 and 22 are the white Duraboard. Photo 316 is conspicuously less accurate: that photo was taken at a more oblique angle and so directional reflectivity effects are likely to explain the discrepancies.

grey samples and photos, or within 5 percent if an average of the three photos is used). The coloured paper samples were rather worse, with errors as much as 30 percentage points seen in one case. The pyromark result was quite good, but only in percentage point terms, as opposed to relative error in reflected energy.

Within the set of grey paper samples, if we refer back to the spectral results for the 410-Solar, it is found that a subset of the grey samples, such as the grey sample in Figure 4, have quite uniform reflectivity out into the infrared wavelengths. For that subset of the coloured samples, the coupon method showed accuracy of ±1.5 percentage points, indicating that much of the error seen in this study is indeed due to the issue outlined in Section 3.2.1.

4. Possible improvements and future work

The evaluation of the coupon method detailed in this paper shows quite accurate results are possible for truly grey surfaces. However, it is clear that a surface which is non-grey, especially in the infrared region, presents a real problem for accurate measurement by this technique. The Pyromark 2500, an example of a CSP receiver coating that is commonly used in practice, shows enough non-grey behaviour for an error of (0.0383-0.0327)/0.0383 = 15% in estimated energy losses to result if non-visible wavelengths are ignored.

Depending on the application, this may or may not be acceptable. If attempting to estimate the absorbed energy for this receiver surface, the error is only (0.0327 - 0.0383) / (1-0.0383) = 0.6%.

The missing information in this approach is the information about longer wavelengths. Actually, CCD and CMOS camera sensors are normally sensitive to longer wavelengths, as shown in Figure 8, but a visible wavelength band-pass filter ('hot mirror') is normally incorporated since the long-wave response produces undesired visual effects in normal photography. One option for low-cost reflectivity measurement might be to attempt to remove this 'hot mirror', and some 'hackers' report success with that approach, at least for obtaining photographs that capture infrared, and not just visible, information.

Another option to increase the accuracy of photographic reflectivity measurement would be to incorporate data from a separate infrared camera. Most of these cameras appear to give proprietary-format images that are calibrated to degrees Celsius, so some calculation would be required to convert that back to an energy value in an appropriate wavelength band. Ideally it should be possible to have a three-band ID camera that makes use of the differences in the CCD channel responses of Figure 8 to give independent information about three different infrared wavelength bands. It has not yet been determined if such cameras are readily or cheaply available.

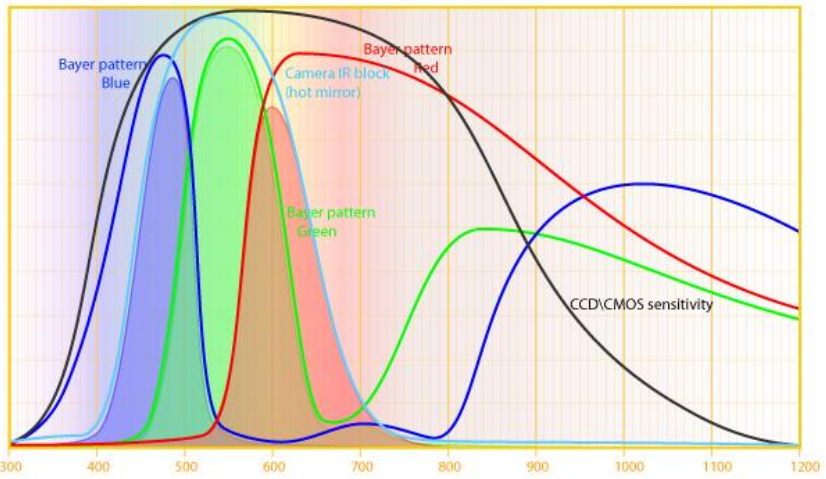

Figure 8. Typical CCD response curve (relative spectral response versus wavelength in nm). The pale blue 'hot mirror' line showns the visible-range light filter which suppresses the response of the CCD to longer-wavelength irradiation (Source:ir-photo.net)

Beyond attempts to characterise reflectivity using infrared photography, it remains to also assess the accuracy of the alternative 'solar' method for calculation of reflectivity and to test these methods on a range of complete solar receivers, rather that the simple planar surfaces used in this study.

5. Conclusion

A simple method for reflectivity measurement using standard DSLR photograph of a reference 'coupon' and a target surface was assessed. The key concern of this method is that it has no information about solar in the infrared band, and that as such an accurate solar-weighted reflectivity measurement is not possible unless the surface being measured is truly 'grey'. The method showed that for truly grey surfaces, reflectivity can be measured to within ±1.5 percentage points, but that the method can be very inaccurate for highly non-grey surfaces. Opportunities to improve this method exist through the addition of infrared photography into the process. Further work will assess this option and assess the accuracy of the 'solar' reflectivity method.

References

[1] S. Meyen, A. Fernandez-Garcia and C. Kennedy, 2011. 'Measurement of solar weighted reflectance of mirror materials for concentrating solar power technology with commercially available instrumentation', Interim Guideline v1.1, SolarPACES, Task III.

[2] C. K. Ho and S. S. Khalsa, 2011. 'A Flux Mapping Method for Central Receiver Systems', *ASME Conference Proceedings* **2011**, 743-751.

[3] C. K. Ho, S. S. Khalsa, D. Gill and C. A. Sims, 2011. 'Evaluation of a New Tool for Heliostat Field Flux Mapping'. In *Proceedings of SolarPACES 2011*, Granada.

[4] A. Hall, A. Ambrosini and C. K. Ho, 2012. 'Solar selective coatings for concentrating solar power central receivers', *Advanced Materials and Processes* **170**, 28-32.

[5] NREL, http://rredc.nrel.gov/solar/spectra/am1.5/ accessed Sept 2012. 'Reference Solar Spectral Irradiance: Air Mass 1.5', ASTM G-173-03, National Renewable Energy Laboratory, Golden, Colorado.